Phys Chem Minerals (1991) 17:554–562

PHYSICS AND CHEMISTRY OF MINERALS

The α-β Phase Transition in Cristobalite, SiO_2

Symmetry Analysis, Domain Structure, and the Dynamical Nature of the β-phase

Dorian M. Hatch[1] **and Subrata Ghose**[2]

[1] Department of Physics, Brigham Young University, Provo, UT 84602, USA
[2] Mineral Physics Group, Department of Geological Sciences, University of Washington, Seattle, WA 98195, USA

Received February 7, 1990

Abstract. Cristobalite, a high temperature phase of silica, SiO_2, undergoes a (metastable) first-order phase transition from a cubic, $Fd\bar{3}m$, to a tetragonal, $P4_32_12$ (or $P4_12_12$), structure at around 220° C. The cubic C9-type structure for β-cristobalite (Wyckoff 1925) is improbable because of two stereochemically unfavorable features: a 180° Si-O-Si angle and an Si-O bond length of 1.54 Å, whereas the corresponding values in tetragonal α-cristobalite are ~146° and 1.609 Å respectively. The structure of the β-phase is still controversial. To resolve this problem, a symmetry analysis of the $Fd\bar{3}m \rightarrow P4_32_12$ (or $P4_12_12$) transition in cristobalite has been carried out based on the Landau formalism and projection operator methods. The starting point is the ideal cubic ($Fd\bar{3}m$) C9-type structure with the unit cell dimension a (7.432 Å) slightly larger than the known a dimension (7.195 Å at 205° C) of β-cristobalite, such that the Si-O-Si angle is still 180°, but the Si-O bond length is 1.609 Å. The six-component order parameter driving the phase transition transforms according to the X_4 representation. The transition mechanism essentially involves a simultaneous translation and rotation of the silicate tetrahedra coupled along ⟨110⟩. A Landau free-energy expression is given as well as a listing of the three types of domains expected in α-cristobalite from the $\beta \rightarrow \alpha$ transition. These domains are: (i) transformation twins from a loss of 3-fold axes, (ii) enantiomorphous twins from a loss of the inversion center, and (iii) antiphase domains from a loss of translation vectors $\frac{1}{2}\langle 110\rangle$ ($F \rightarrow P$). These domains are macroscopic and static in α-cristobalite, and microscopic and dynamic in β-cristobalite. The order parameter η, couples with the strain components as $\varepsilon\eta^2$, which initiates the structural fluctuations, thereby causing the domain configurations to dynamically interchange in the β-phase. Hence, the α-β cristobalite transition is a fluctuation-induced first-order transition and the β-phase is a dynamic average of α-type domains.

Introduction

The high temperature phase of silica, SiO_2, stable between 1470° C and the melting point 1728° C, is known as β-cristobalite (Fig. 1) which persists metastably down to about 275° C and inverts to the low temperature phase α-cristobalite (Fig. 2). The α-β phase transition is rapid and reversible, but shows a strong hysteresis effect and is first-order (see e.g. Leadbetter and Wright 1976). The structure of α-cristobalite (tetragonal, $P4_32_12$

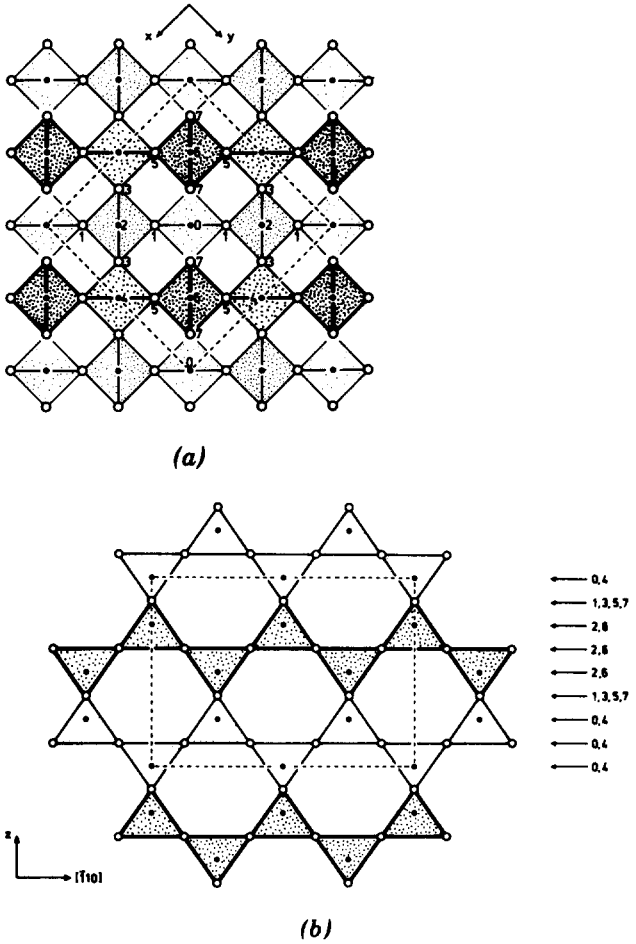

Fig. 1a, b. Ideal C9 structure (cubic, $Fd\bar{3}m$) of β-cristobalite; (**a**) projection on (001), (**b**) on (110). Small filled circles are Si atoms and large open circles are oxygen atoms. Heights are in multiples of $c/8$ or $a[110]/8$ (reproduced from O'Keefe and Hyde 1976)

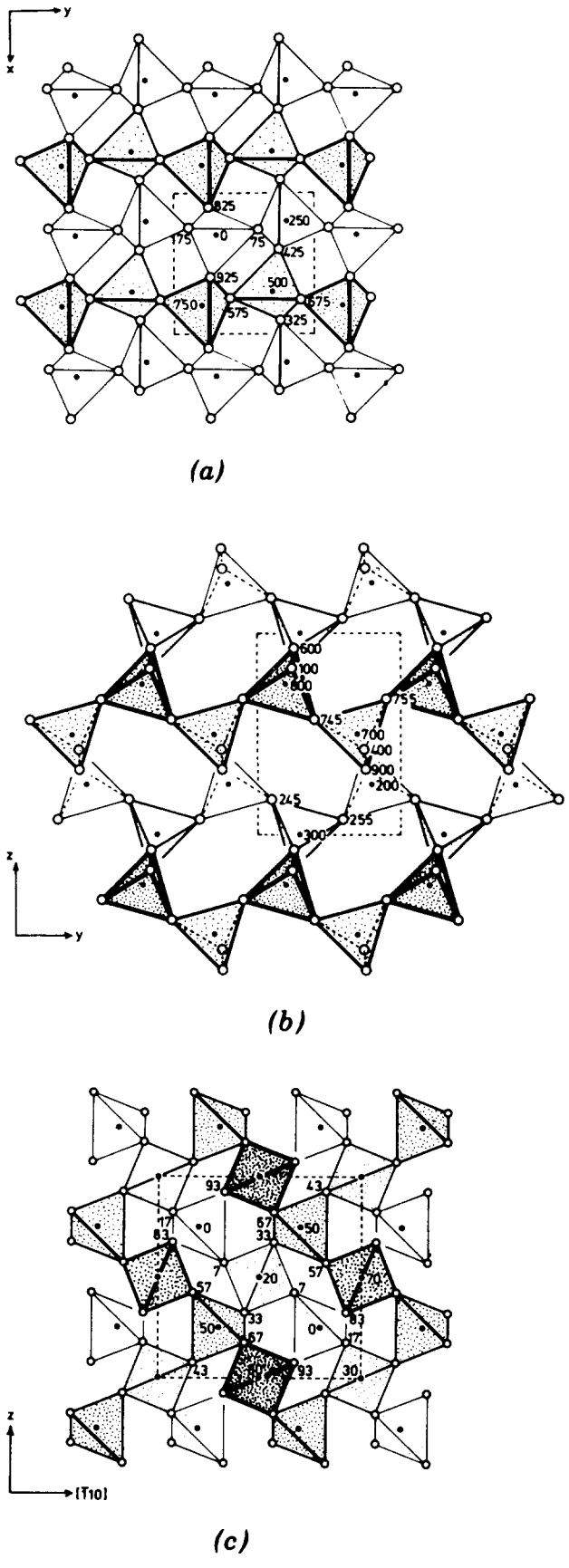

Fig. 2. The structure of α-cristobalite (tetragonal, $P4_12_12$) in three projections: (**a**) on (001), (**b**) on (100), and (**c**) on (110) of the $P4_12_12$ cell. Heights are in multiples of 0.001 × the appropriate axis (reproduced from O'Keefe and Hyde 1976)

or $P4_12_12$; $a=4.98$ Å, $c=6.95$ Å) is well established from single crystal x-ray diffraction studies (Dollase 1965; Peacor 1973). However, in spite of a long history of investigations on the α-β cristobalite transition, the nature of the β-phase (cubic, $Fd\bar{3}m$; $a=7.14$ Å) is highly controversial and the details of the microscopic transition mechanism are unknown. Based on high temperature x-ray powder diffraction, Wyckoff (1925) first proposed a structure of β-cristobalite (C9 type), where 8 silicon atoms are located in 8(a) $(\frac{1}{8}, \frac{1}{8}, \frac{1}{8})$, $\circlearrowleft$ (site symmetry $\bar{4}3m$) and 16 oxygen atoms in 16(c) (0,0,0), $\circlearrowleft$ (site symmetry $\bar{3}$m). (Origin choice 2 for $Fd\bar{3}m$ in International Tables for Crystallography (1983) has been chosen.) It was soon realized, however, that the C9 structure (Fig. 1) cannot be correct in detail (Nieuwenkamp 1937). In this structure, the oxygen atom located between two silicon atoms along the Si-Si axis parallel to ⟨111⟩ requires the Si-O-Si angle to be 180° and the Si-O bond length 1.54 Å; these values are highly improbable if we assume the silicate tetrahedra to behave as rigid groups through the transition since the corresponding values in α-cristobalite are 146° and 1.609 Å. To circumvent this problem, Nieuwenkamp (1937) proposed that the oxygen atom is displaced from the 16(c) position normal to the Si-Si axis and is rotating in a small circle with a radius of ~0.4 Å normal to ⟨111⟩; this implies a hindered rotation of the silicate tetrahedra. Nieuwenkamp pointed out that from the x-ray diffraction evidence, this model is indistinguishable from a statistical six-fold or twelve-fold disorder in which the oxygen atoms occupy the 96(h) or 192(i) positions respectively. Subsequent workers adopted the disordered 96(h) structure for the oxygen atoms which substantially improved the agreement between calculated and observed x-ray intensities over the C9 structure (Peacor 1973; Wright and Leadbetter 1975). The oxygen atoms in the 96(h) positions require one-sixth occupancy at each of the six positions separated by a rotation of 60° on a small circle with a radius of 0.45 Å around the Si-Si axis, resulting in a Si-O bond length of 1.609 Å and Si-O-Si angle, 146°. The structure of β-cristobalite was interpreted as an average of six domains around each ⟨111⟩ axis of the cubic phase. Peacor (1973) favored a structure where the domains are dynamically changing configurations. However, on the basis of x-ray evidence alone, it was not possible to determine whether the domains are static or dynamic. From these studies, it is not at all obvious why the high temperature β-phase should contain twin domains, whereas the low temperature α-phase can occur in nature as single octahedral crystals without twinning (Van Valkenburg, Jr. and Buie 1945). To complicate the issue further, Wright and Leadbetter (1975) proposed the symmetry of the twin domains in the β-phase to be $I\bar{4}2d$, which is not a supergroup of $P4_32_12$ (or $P4_12_12$). O'Keefe and Hyde (1976) also considered the symmetry of the domains in the β-phase to be $I\bar{4}2d$. In their view, β-cristobalite is a partially collapsed form of the C9 structure, thereby reducing the symmetry from $Fd\bar{3}m$ to $I\bar{4}2d$, brought about by a combination of tilt/rotation of each tetrahedron about parallel $\bar{4}$ axes, alternately clockwise and anticlockwise, so that the tetrahe-

dral corner-sharing connectivity is retained. They proposed a transition mechanism from $I\bar{4}2d$ (β-phase) to $P4_12_12$ (α-phase) by further tetrahedral rotations (see Fig. 14, O'Keefe and Hyde 1976). Tetrahedral rotation modes leading from the C9 structure to α-cristobalite were derived by Fischer and Zemann (1975) and O'Keefe and Hyde (1976). Lally et al. (1978) found the displacement vector for the antiphase domains in α-cristobalite from lunar samples in the electron microscope to be $\frac{1}{2}\langle 111\rangle$, which they believed to be a confirmation of the $I\bar{4}2d \rightarrow P4_32_12$ transition.

Hua et al. (1988) observed strong diffuse scattering in electron diffraction patterns of the β-phase and suggested that the α-β transition is dynamic. The diffuse scattering occurs in planes in reciprocal space normal to six $\langle 110\rangle$ directions of the cubic $Fd\bar{3}m$ cell, indicating the presence of columnar domains, a few unit cells thick, parallel to $\langle 110\rangle$. Their lattice dynamical study of β-cristobalite based on the C9 structure gave a satisfactory explanation of the diffuse scattering, but did not give atomic displacements large enough to be consistent with the 146° Si-O-Si angle. A Monte Carlo simulation with the Si-O-Si angle constrained to 146° showed that the oxygen atoms are distributed *uniformly* around an annulus encircling the 16(c) sites of the $Fd\bar{3}m$ C9 structure (Welberry et al. 1989), contradicting the x-ray diffraction results, but consistent with the earlier view of Nieuwenkamp (1937) that the oxygen atoms are rotating around 16(c) sites. In a subsequent paper, Withers et al. (1989) proposed tetrahedral rotational modes (R_{14}) in the C9 structure, which are responsible for the $\beta \rightarrow \alpha$ transition and the resulting microstructure in low cristobalite. In summary, the x-ray and electron diffraction studies on α- and β-cristobalite do not yield a convincing picture of the microscopic mechanism of the phase transition and the nature of β-cristobalite.

In this paper, we present a symmetry analysis of the $Fd\bar{3}m \rightarrow P4_32_12$ (or $P4_12_12$) transition in cristobalite based on a Landau-type formalism and projection operator methods. Our starting point is the ideal cubic ($Fd\bar{3}m$) C9 structure with the unit cell dimension, a (7.432 Å) slightly larger than the known a dimension (7.195 Å at 205° C) of β-cristobalite, such that the Si-O-Si angle is still 180°, but the Si-O bond length (1.609 Å) corresponds to that in α-cristobalite (Dollase 1965). We show that the transition $\beta \rightarrow \alpha$ involves simultaneous rotation and translation of the silicate tetrahedra resulting in a collapse of the ideal β-structure to the α-structure and a simultaneous change in the Si-O-Si angle from the ideal 180° value to 146°. We show further that the order parameter driving the phase transition transforms according to the X_4 representation (labeling of Miller and Love 1967). In addition to a Landau free energy expression, we list the detailed configurations of the three types of microstructures to be expected in α-cristobalite from the $\beta \rightarrow \alpha$ transition, namely, (i) transformation twins from the loss of the three-fold rotation axes $\langle 111\rangle$; (ii) enantiomorphic twins from the loss of the center of inversion, and (iii) antiphase domains from the loss of the translation vectors $\frac{1}{2}\langle 110\rangle$ ($F \rightarrow P$). We show that the various configurations of these three types of domains, giving the average symmetry $Fd\bar{3}m$, result in a disordered structure, where the 8 silicon atoms are still in 8(a), but each of the 16 oxygen atoms are distributed in 96(h) positions at the corners of a hexagon around the 16(c) positions with one-sixth occupancy at each site. This view is consistent with the structural model proposed earlier for the β-phase based on x-ray diffraction (Peacor 1973; Wright and Leadbetter 1975). The intrinsic symmetry of these domains in the high temperature phase is $P4_32_12$ (or $P4_12_12$) and not $I\bar{4}2d$ as proposed by some investigators (Wright and Leadbetter 1975; O'Keefe and Hyde 1976).

These P-type domains are static and large (macroscopic) in the α-phase and dynamic and microscopic in the β-phase. The order parameter couples with the strain components, which transform as the Γ_1^+ and Γ_3^+ representations. It is the order parameter-strain coupling which initiates the structural fluctuations, causing the domain configurations to dynamically interchange in the β-phase. Hence, the α-β cristobalite transition is a fluctuation-induced first-order phase transition and the β-cristobalite is a dynamic average of α-cristobalite type domains. This view is consistent with all experimental evidence available so far on both α- and β-cristobalite.

Symmetry Analysis of the Phase Transition and the Expected Domain Configurations in the Low Temperature Phase

It is generally agreed by all investigators that the average structure of the high cristobalite phase is represented by the space group symmetry $Fd\bar{3}m$ (O_h^7). For the ideal β-cristobalite structure (the C9 structure of Wyckoff, 1925) the silicon atoms are located on 8(a) sites while the oxygens are on 16(c) sites, resulting in a 180° Si-O-Si bond angle (Fig. 1). The β-α transition then brings about a lowering of symmetry to space group $P4_32_12$ (D_4^8) (or its enantiomorph $P4_12_12$ (D_4^4)). The tables by Stokes and Hatch (1988) contain the results of group theoretical methods applied to the analysis of group-subgroup transitions for all 230 space groups. From Table 1 of that work it is seen that irreducible representations X_3, X_4, W_1 and W_2 of $Fd\bar{3}m$ (notation of Miller and Love 1967) all lead to structures which have space group symmetry $P4_32_12$. However, only X_4 leads to a structure with a primitive cell size doubling, consistent with the experimental description of the lower symmetry α phase. (See Fig. 3 for the location of points in the Brillouin Zone.) Thus the X_4 representation is the appropriate representation on which we base our development. A great deal of information about the description of the $Fd\bar{3}m$ to $P4_32_12$ transition can be obtained by using the results listed in the tables by Stokes and Hatch (1988). The information given there will be used in this discussion. The interested reader can refer to those tables for additional details.

The X_4 irreducible representation is a six-dimensional representation, two dimensions arising from each of the three symmetry related **X**-points $(0, 0, \frac{1}{2})$, $(0, \frac{1}{2}, 0)$, $(\frac{1}{2}, 0, 0)$ in terms of conventional lattice vectors in recip-

Table 1. The twelve domains resulting from the $Fd\bar{3}m$ to $P4_32_12$ transition

	Direction	Basis (Handedness)	Origin
(1)	(a, a, 0, 0, 0, 0)	$(\frac{1}{2}, \frac{1}{2}, 0)$ $(-\frac{1}{2}, \frac{1}{2}, 0)$ (0, 0, 1) (r.h.)	$(-\frac{1}{8}, \frac{1}{8}, \frac{3}{8})$
(2)	(0, 0, 0, 0, a, a)	$(\frac{1}{2}, 0, \frac{1}{2})$ $(\frac{1}{2}, 0, -\frac{1}{2})$ (0, 1, 0) (r.h.)	$(\frac{1}{8}, \frac{3}{8}, -\frac{1}{8})$
(3)	(0, 0, a, a, 0, 0)	$(0, \frac{1}{2}, \frac{1}{2})$ $(0, -\frac{1}{2}, \frac{1}{2})$ (1, 0, 0) (r.h.)	$(\frac{3}{8}, -\frac{1}{8}, \frac{1}{8})$
(4)	(−a, a, 0, 0, 0, 0)	$(-\frac{1}{2}, -\frac{1}{2}, 0)$ $(\frac{1}{2}, -\frac{1}{2}, 0)$ (0, 0, −1) (l.h.)	$(\frac{1}{8}, -\frac{1}{8}, -\frac{3}{8})$
(5)	(0, 0, 0, 0, −a, a)	$(-\frac{1}{2}, 0, -\frac{1}{2})$ $(-\frac{1}{2}, 0, \frac{1}{2})$ (0, −1, 0) (l.h.)	$(-\frac{1}{8}, -\frac{3}{8}, \frac{1}{8})$
(6)	(0, 0, −a, a, 0, 0)	$(0, -\frac{1}{2}, -\frac{1}{2})$ $(0, \frac{1}{2}, -\frac{1}{2})$ (−1, 0, 0) (l.h.)	$(-\frac{3}{8}, \frac{1}{8}, -\frac{1}{8})$
(7)	(−a, −a, 0, 0, 0, 0)	$(\frac{1}{2}, \frac{1}{2}, 0)$ $(-\frac{1}{2}, \frac{1}{2}, 0)$ (0, 0, 1) (r.h.)	$(-\frac{1}{8}, \frac{5}{8}, \frac{7}{8})$
(8)	(0, 0, 0, 0, −a, −a)	$(\frac{1}{2}, 0, \frac{1}{2})$ $(\frac{1}{2}, 0, -\frac{1}{2})$ (0, 1, 0) (r.h.)	$(\frac{5}{8}, \frac{7}{8}, -\frac{1}{8})$
(9)	(0, 0, −a, −a, 0, 0)	$(0, \frac{1}{2}, \frac{1}{2})$ $(0, -\frac{1}{2}, \frac{1}{2})$ (1, 0, 0) (r.h.)	$(\frac{7}{8}, -\frac{1}{8}, \frac{5}{8})$
(10)	(a, −a, 0, 0, 0, 0)	$(-\frac{1}{2}, -\frac{1}{2}, 0)$ $(\frac{1}{2}, -\frac{1}{2}, 0)$ (0, 0, −1) (l.h.)	$(\frac{1}{8}, -\frac{5}{8}, -\frac{7}{8})$
(11)	(0, 0, 0, 0, a, −a)	$(-\frac{1}{2}, 0, -\frac{1}{2})$ $(-\frac{1}{2}, 0, \frac{1}{2})$ (0, −1, 0) (l.h.)	$(-\frac{5}{8}, -\frac{7}{8}, \frac{1}{8})$
(12)	(0, 0, a, −a, 0, 0)	$(0, -\frac{1}{2}, -\frac{1}{2})$ $(0, \frac{1}{2}, -\frac{1}{2})$ (−1, 0, 0) (l.h.)	$(-\frac{7}{8}, \frac{1}{8}, -\frac{5}{8})$

In the table are listed for each domain the domain number, the non-zero components of the order parameter, the subgroup lattice vectors defined in terms of the conventional basis vectors of $Fd\bar{3}m$, the basis handedness, and the subgroup origin relative to the origin of $Fd\bar{3}m$

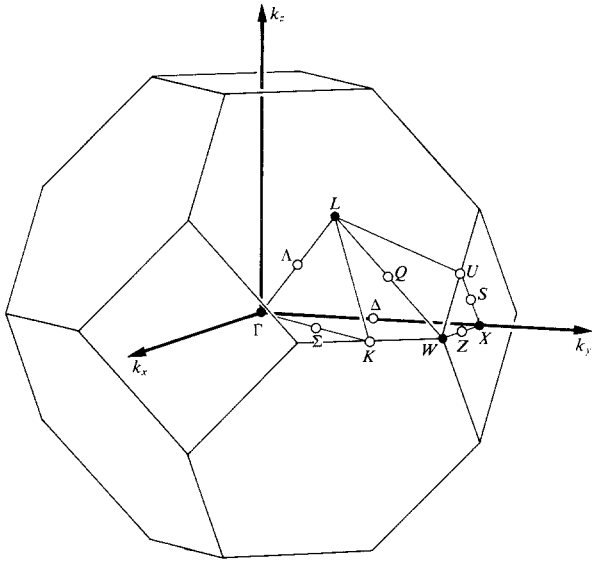

Fig. 3. Brillouin zone for the face centered space group $Fd\bar{3}m$. The location of the **X**-point used for the description of the $Fd\bar{3}m$ to $P4_32_12$ transition is shown; $\mathbf{X}=(0, \frac{1}{2}, 0)$ (reproduced from Miller and Love 1967)

rocal space. The components of the order parameter $\eta=(\eta_1, \eta_2, \eta_3, \eta_4, \eta_5, \eta_6)$ serve as a basis for the irreducible representation. The X_4 irreducible representation does not allow the construction of a Landau third order invariant nor a Lifshitz invariant. Using these results and minimizing the free energy it is found that the β-α transition is allowed to be continuous within Landau theory. However, renormalization group methods indicate that there are no stable fixed points and therefore the transition will be a first-order transition due to fluctuations-a so-called fluctuation-induced first-order transition. The transition is classified as *improper ferroelastic* which means that the components of strain cannot transform in the same manner as the primary order parameter components, i.e. the transformation properties of strain are not given by the X_4 representation. Hence, any spontaneous strain contributions due to the transition must result from a coupling with the primary order parameter X_4. According to Stokes and Hatch (1988) the $P4_32_12$ subgroup results from the onset of an order parameter of the form $\eta=(a, a, 0, 0, 0, 0)$. This gives a domain, domain (1), in which $P4_32_12$ has tetragonal lattice vectors $\mathbf{a}_t=(\frac{1}{2}, \frac{1}{2}, 0)$, $\mathbf{b}_t=(\frac{1}{2}, -\frac{1}{2}, 0)$ and $\mathbf{c}_t=(0, 0, 1)$, where $\mathbf{a}_t$, $\mathbf{b}_t$, and $\mathbf{c}_t$ are given in terms of the conventional lattice vectors of the cubic $Fd\bar{3}m$ phase. The origin of the $P4_32_12$ subgroup is at $(-\frac{1}{8}, \frac{1}{8}, \frac{3}{8})$ relative to the origin of $Fd\bar{3}m$. In this discussion the origin choice 2 is used for $Fd\bar{3}m$ (International Tables for Crystallography v.A., 1983), which is the same one used by Peacor (1973).

During the transition from $Fd\bar{3}m$ to $P4_32_12$ a set of symmetry elements is lost. As a result, several domains with equivalent space group symmetry are possible but with different orientations relative to the high symmetry $Fd\bar{3}m$ structure. In Table 1 are listed twelve domains resulting from the transition to $P4_32_12$. Each domain has a different orientation but the same structural (space group) symmetry $P4_32_12$. In that table the following information is given: the domain number, the components of the order parameter for each domain, the lattice basis vectors for the subgroup of that domain, the handedness of the basis, and the subgroup origin relative to the origin of $Fd\bar{3}m$. The space group of each domain is in a specific subgroup relationship to $Fd\bar{3}m$ and they are therefore in a well defined relationship to each other. They are conjugate subgroups relative to $Fd\bar{3}m$ with the conjugacy element being a symmetry element of $Fd\bar{3}m$ not contained in $P4_32_12$. For example, the symmetry element relating to (x, y, z) to (z, x, y) is a three-fold rotation about the axis [111] of the cubic phase. The rotation is not an element of the $P4_32_12$ structure of domain (1). It transforms the order parameter (a, a, 0, 0, 0, 0) to the direction (0, 0, a, a, 0, 0) and gives the conjugate subgroup for domain (3). If **R** represents the three-fold rotation, $(P4_32_12)_{\text{Dom 3}}=\mathbf{R}$ $(P4_32_12)_{\text{Dom 1}}$ $\mathbf{R}^{-1}$ indicates the relationship of the symmetry groups of these two domains. The first three domains of Table 1 are transformation twins related by three-fold rotations along $\langle 111 \rangle$ directions. Domain (7) is related to domain (1) by the lost symmetry element

of translation by $(0, \frac{1}{2}, \frac{1}{2})$ due to the transition from F to P lattice. This element is in $Fd\bar{3}m$ but is not a symmetry element of $P4_32_12$ of domain (1). As can be seen from the origin column of Table 1, domains (7), (8), and (9) are related to (1), (2), and (3) by the lost translations $(0, \frac{1}{2}, \frac{1}{2})$, $(\frac{1}{2}, \frac{1}{2}, 0)$ and $(\frac{1}{2}, 0, \frac{1}{2})$ respectively. These domains are in an antiphase relationship. For the six remaining domains there is the notation l.h. or left handed. All domains have been described in the space group $P4_32_12$ which does not contain the inversion transformation (x, y, z) to $(\bar{x}, \bar{y}, \bar{z})$, which exists in $Fd\bar{3}m$. As a result, a left-handed set of lattice vectors was used; this is seen from the specification of the lattice vectors in the table. The $P4_32_12$ structure of these domains can be just as well described in a right-handed coordinate system, obtained by inverting the directions of the basis vectors. This results in the subgroup $P4_12_12$. Thus, the six left-handed $P4_32_12$ domains are enantiomorphous to six right-handed domains if described by the space group $P4_12_12$.

From Tables 9 and 10 of Stokes and Hatch (1988) the invariant polynomials of the primary order parameter η in the free energy expansion can be obtained. In Eq. (1) the free energy to fourth degree is reproduced from those tables,

$$\begin{aligned}\Delta F = & a(\eta_1^2+\eta_2^2+\eta_3^2+\eta_4^2+\eta_5^2+\eta_6^2)\\ & +b(\eta_1^2+\eta_2^2+\eta_3^2+\eta_4^2+\eta_5^2+\eta_6^2)^2\\ & +c(\eta_1^4+\eta_2^4+\eta_3^4+\eta_4^4+\eta_5^4\eta_6^4)\\ & +d(\eta_1^2\eta_2^2+\eta_3^2\eta_4^2+\eta_5^2\eta_6^2)\\ & +e(\eta_1\eta_2\eta_3\eta_4+\eta_1\eta_2\eta_5\eta_6+\eta_3\eta_4\eta_5\eta_6) \qquad (1)\end{aligned}$$

where a, b, c, d, and e are Landau coefficients.

At the phase transition the order parameter becomes non-zero, which reduces the symmetry of the structure to the subgroup $P4_32_12$ of $Fd\bar{3}m$. The order parameter η=(a, a, 0, 0, 0, 0) minimizes the free energy for $T<T_c$. Since the free energy is invariant under elements of $Fd\bar{3}m$, the elements which relate the order parameter of the domains listed in Table I give the same free energy values for each domain. Thus the order parameter value for each domain gives the same free energy value and thus each minimizes the free energy. The domains give equal energy minima of ΔF.

Rotational Microscopic Distortions

The discussion of the transition to this point has used general symmetry properties associated with the transition; the order parameter transforming according to the irreducible representation X_4 and the subgroup $P4_32_12$ results when η takes the form η=(a, a, 0, 0, 0, 0). In β-cristobalite the average positions for Si are the 8(a) positions $\frac{1}{8}, \frac{1}{8}, \frac{1}{8}$ ∪ and for O the 16(c) (0, 0, 0), ∪ positions. In silica polymorphs the tetrahedral silicate group [SiO_4] behaves as a rigid group at relatively low temperatures. Assuming a rigid tetrahedron around each Si, the order parameter is initially taken to be a rotation of these tetrahedra. The order parameter η=(a, a, 0, 0, 0, 0) of the X_4 irreducible representation then demands a specific rotational distortion away from the symmetric $Fd\bar{3}m$ structure. By projection operator techniques the rotational displacement patterns can be explicitly obtained. In Table 2 are shown the axial vector (rotation) components of the tetrahedra about the silicon centers for the six components (modes) of the order parameter transforming according to X_4. The entries in the table indicate the axial vector components around the two silicon atoms near (0, 0, 0), the two around the centered point $(0, \frac{1}{2}, \frac{1}{2})$, etc. Thus for mode (1) (η=(1, 0, 0, 0, 0, 0)) the tetrahedron about the Si atom at $(\frac{1}{8}, \frac{1}{8}, \frac{1}{8})$ rotates a certain amount (right hand rotation) around the [1, −1, 0] direction, the tetrahedron around the Si atom at $(\frac{7}{8}, \frac{3}{8}, \frac{3}{8})$ rotates the same amount around [1, −1, 0] the tetrahedron centered at $(\frac{1}{8}, \frac{5}{8}, \frac{5}{8})$ rotates the same amount around [−1, 1, 0] and so on.

Table 2. The six axial vector (rotation) mode components for the rigid SiO_4 tetrahedra.

Mode	Points $(\frac{1}{8}, \frac{1}{8}, \frac{1}{8})$ $(\frac{7}{8}, \frac{3}{8}, \frac{3}{8})$	Points $(\frac{1}{8}, \frac{5}{8}, \frac{5}{8})$ $(\frac{7}{8}, \frac{7}{8}, \frac{7}{8})$	Points $(\frac{5}{8}, \frac{1}{8}, \frac{5}{8})$ $(\frac{3}{8}, \frac{3}{8}, \frac{7}{8})$	Points $(\frac{5}{8}, \frac{5}{8}, \frac{1}{8})$ $(\frac{3}{8}, \frac{7}{8}, \frac{3}{8})$
1	(1, −1, 0)	(−1, 1, 0)	(−1, 1, 0)	(1, −1, 0)
	(1, −1, 0)	(−1, 1, 0)	(−1, 1, 0)	(1, −1, 0)
2	(1, 1, 0)	(−1, −1, 0)	(−1, −1, 0)	(1, 1, 0)
	(−1, −1, 0)	(1, 1, 0)	(1, 1, 0)	(−1, −1, 0)
3	(0, 1, −1)	(0, 1, −1)	(0, −1, 1)	(0, −1, 1)
	(0, −1, 1)	(0, −1, 1)	(0, 1, −1)	(0, 1, −1)
4	(0, 1, 1)	(0, 1, 1)	(0, −1, −1)	(0, −1, −1)
	(0, 1, 1)	(0, 1, 1)	(0, −1, −1)	(0, −1, −1)
5	(−1, 0, 1)	(1, 0, −1)	(−1, 0, 1)	(1, 0, −1)
	(−1, 0, 1)	(1, 0, −1)	(−1, 0, 1)	(1, 0, −1)
6	(1, 0, 1)	(−1, 0, −1)	(1, 0, 1)	(−1, 0, −1)
	(−1, 0, −1)	(1, 0, 1)	(−1, 0, −1)	(1, 0, 1)

The rotational modes transform according to the six-dimensional X_4 irreducible representation. The numbers in parenthesis for each mode indicate the relative mangitudes of the components along $\mathbf{a}_c$, $\mathbf{b}_c$, and $\mathbf{c}_c$. Each of the eight silicon atoms listed (points) are at the center of tetrahedra and the latter rotate in the manner listed in the table

At the transition to $P4_32_12$ (domain (1)) the order parameter η=(a, a, 0, 0, 0, 0) has equal contributions from the first two modes and zero contributions from the other four. Adding the first two modes gives (2a, 0, 0), (0, −2a, 0), (−2a, 0, 0) (0, 2a, 0), (−2a, 0, 0), (0, 2a, 0), (2a, 0, 0) and (0, −2a, 0). This order parameter distortion gives rotations of equal amounts around the [1, 0, 0] direction for the tetrahedron centered at $(\frac{1}{8}, \frac{1}{8}, \frac{1}{8})$, around [0, −1, 0] for the tetrahedron at $(\frac{7}{8}, \frac{3}{8}, \frac{3}{8})$, around [−1, 0, 0] for the tetrahedron centered at $(\frac{1}{8}, \frac{5}{8}, \frac{5}{8})$, etc. This rotational pattern is shown in Fig. 4(a). The rotational mode for the enantiomorphic twin domain (4), is (0, 2a, 0), (−2a, 0, 0), (0, −2a, 0), (2a, 0, 0), (0, −2a, 0), (2a, 0, 0), (0, 2a, 0), (−2a, 0, 0) and is shown in Fig. 4(b). The rotational mode patterns for the other domains can be obtained in a similar manner. By using Figs. 1 and 4 it is seen that the rotational mode for domain (a) consists of alternating orthogonal rotations (e.g., around [1, 0, 0] and then

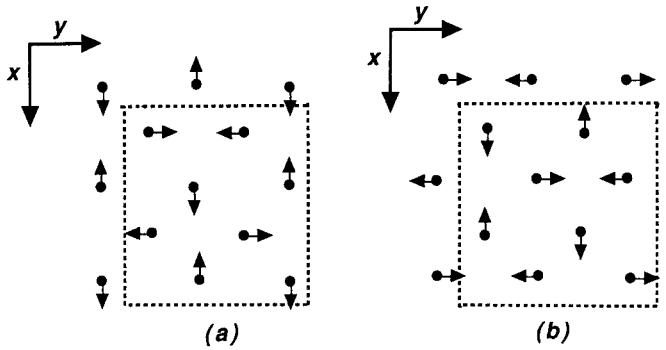

Fig. 4. (**a**) Rotational mode pattern of rigid tetrahedra coordinating silicon atoms resulting in the subgroup $P4_32_12$, domain (1). Axial vectors are located at the 8(a) silicon positions of $Fd\bar{3}m$. The vectors indicate the direction of the right-handed rotation axis. (**b**) Rotational mode pattern for domain (4) of left-handed $P4_32_12$, which is enantiomorphic to $P4_12_12$

Table 3. The rotational modes producing six of the twelve domains resulting from the $Fd\bar{3}m$ to $P4_32_12$ transition

Domain	Points $(\frac{1}{8}, \frac{1}{8}, \frac{1}{8})$ $(\frac{7}{8}, \frac{3}{8}, \frac{3}{8})$	Points $(\frac{1}{8}, \frac{5}{8}, \frac{5}{8})$ $(\frac{7}{8}, \frac{7}{8}, \frac{7}{8})$	Points $(\frac{5}{8}, \frac{1}{8}, \frac{5}{8})$ $(\frac{3}{8}, \frac{3}{8}, \frac{7}{8})$	Points $(\frac{5}{8}, \frac{5}{8}, \frac{1}{8})$ $(\frac{3}{8}, \frac{7}{8}, \frac{3}{8})$
(1)	(2a, 0, 0) (0, −2a, 0)	(−2a, 0, 0) (0, 2a, 0)	(−2a, 0, 0) (0, 2a, 0)	(2a, 0, 0) (0, −2a, 0)
(2)	(0, 0, 2a) (−2a, 0, 0)	(0, 0, −2a) (2a, 0, 0)	(0, 0, 2a) (−2a, 0, 0)	(0, 0, −2a) (2a, 0, 0)
(3)	(0, 2a, 0) (0, 0, 2a)	(0, 2a, 0) (0, 0, 2a)	(0, −2a, 0) (0, 0, −2a)	(0, −2a, 0) (0, 0, −2a)
(4)	(0, 2a, 0) (−2a, 0, 0)	(0, −2a, 0) (2a, 0, 0)	(0, −2a, 0) (2a, 0, 0)	(0, 2a, 0) (−2a, 0, 0)
(5)	(2a, 0, 0) (0, 0, −2a)	(−2a, 0, 0) (0, 0, 2a)	(2a, 0, 0) (0, 0, −2a)	(−2a, 0, 0) (0, 0, 2a)
(6)	(0, 0, 2a) (0, 2a, 0)	(0, 0, 2a) (0, 2a, 0)	(0, 0, −2a) (0, −2a, 0)	(0, 0, −2a) (0, −2a, 0)

The mode for each domain is made up of two of the modes in Table 2. (See Table 2 for further explanation

[0, 1, 0]) of tetrahedra connected along the [1, 1, 0] and [1, −1, 0] chains. The direction of the rotations as one moves from one [1, 1, 0] chain to a neighboring [1, 1, 0] chain results in a primitive cell size of two at the transition. Rotational modes for the six domains are shown in Table 3. The other six domain modes are obtained by reversing the signs on the rotation vectors.

Relationship of the Domain to the Disordered Structure

In $Fd\bar{3}m$ the Si atoms are in 8(a) positions and the oxygen atoms are in 16(c) positions. Hence, for the specific silicon atom at $(\frac{1}{8}, \frac{1}{8}, \frac{1}{8})$, the coordinating oxygens are at *relative* positions $(-\frac{1}{8}, -\frac{1}{8}, -\frac{1}{8})$, $(\frac{1}{8}, -\frac{1}{8}, \frac{1}{8})$, $(\frac{1}{8}, \frac{1}{8}, -\frac{1}{8})$ and $(-\frac{1}{8}, \frac{1}{8}, \frac{1}{8})$. As can be seen from Table 3 the twelve domains resulting from the phase transition are characterized by rotations around the three orthogonal axes along $\mathbf{a}_c$, $\mathbf{b}_c$, and $\mathbf{c}_c$, for each axis they can be in a positive or negative sense (direction). Assume that at the transition a rotation about a specific silicon atom is around the $\mathbf{a}_c$ axis (for example the silicon at $(\frac{1}{8}, \frac{1}{8}, \frac{1}{8})$ for domain (1)). Then a rotation of angle θ around $\mathbf{a}_c$ takes the oxygen at *relative* position $(-\frac{1}{8}, -\frac{1}{8}, -\frac{1}{8})$ to $(-\frac{1}{8}, -c\frac{1}{8}, +s\frac{1}{8}, -s\frac{1}{8}, -c\frac{1}{8})$, where $c \equiv \cos\theta$, and $s \equiv \sin\theta$. A rotation of $-\theta$ results in the relative position $(-\frac{1}{8}, -c\frac{1}{8}, -s\frac{1}{8}, +s\frac{1}{8}, -c\frac{1}{8})$. For rotations around $\mathbf{b}_c$ and $\mathbf{c}_c$ one obtains $(-c\frac{1}{8}, \pm s\frac{1}{8}, -\frac{1}{8}, \mp s\frac{1}{8}, -c\frac{1}{8})$ and $(-c\frac{1}{8} \mp s\frac{1}{8}, \pm s\frac{1}{8}, -c\frac{1}{8}, -\frac{1}{8})$ respectively. From the experimentally derived oxygen atom coordinates given by Peacor (1973), $\theta \approx 16°$ and thus lowest order expansions of $\cos\theta$ and $\sin\theta$ are good approximations. Then the six atomic positions of the oxygen at the relative position $(-\frac{1}{8}, -\frac{1}{8}, -\frac{1}{8})$ for the 12 domains are $(0, \mp\frac{\theta}{8}, \pm\frac{\theta}{8})$, $(\mp\frac{\theta}{8}, 0, \pm\frac{\theta}{8})$, and $(\pm\frac{\theta}{8}, \mp\frac{\theta}{8}, 0)$. These six positions correspond to the 96(h) points with $(\frac{\theta}{8}$ radians) being the value of y in the International Tables for Crystallography v. A (1983). This, then, is the basis for the relative success of the x-ray refinement of the high temperature $Fd\bar{3}m$ structure using a disordered 96(h) model for the oxygen atom (Nieuwenkamp 1937; Peacor 1973; Wright and Leadbetter 1975), which implies that β-cristobalite is an average (static or dynamic) of α-cristobalite-type domains. The nature of the β-phase will be discussed later in greater detail.

From the determinations made by Sapriel (1975), the orientations of domain walls between the transformation twins is crystallographically fixed by the high symmetry groups $Fd\bar{3}m$. Under the listing 432F422 of his Table 1 is given the domain wall relations $x=y$, $y=z$, $z=x$, $x=-y$, $y=-z$, and $z=-$x. Thus the transformation twin boundaries of α-cristobalite will be diagonal {110} planes containing one axis and making 45° angles with the other two. The relationship of the antiphase and enantiomorphic domains is not fixed crystallographically and hence the walls between these domains can be irregular.

Additional Distortions Contributing to the Primary Order Parameter

Up to this point the discussion has emphasized the tetrahedral rotational modes transforming according to the X_4 irreducible representation. For the domain considerations made earlier the rotations were about fixed 8(a) positions of $Fd\bar{3}m$. The justification was the assumed nearly rigid tetrahedra around each silicon atom. Continuing with this same assumption, it is possible to have additional displacements of the centers of mass of the tetrahedra, i.e., silicon atom displacements. The Si-displacement mode pattern is the same as that given in Tables 2 and 3, except that the axial vectors of rotation are now to be interpreted as the polar vectors of the Si-displacements. Thus for domain (1) the silicon atom displacements are $(x, 0, 0)$, $(0, -x, 0)$, $(-x, 0, 0)$, $(0, x, 0)$, $(-x, 0, 0)$, $(0, x, 0)$, $(x, 0, 0)$ and $(0, -$x$x, 0)$. A more complete distortional mode at the transition would consist of a contribution from the rotational mode *and* the displacement mode. The amount of each mode cannot be determined by symmetry but rather by

a lattice dynamical calculation incorporating microscopic potentials.

Coupling of the Primary Order Parameter with Spontaneous Strain

In the transition from $Fd\bar{3}m$ the onset of the primary order parameter $\eta = (a, a, 0, 0, 0, 0)$ determines the lower symmetry $P4_32_12$. At the transition there are additional distortions which are expected to occur. These will be referred to as secondary order parameters. Of particular interest is the accompanying spontaneous strain (Aizu 1970). For the transition to $P4_32_12$, strain components transforming under the one-dimensional irreducible representation Γ_1^+ and the two dimensional irreducible representation Γ_3^+ both occur and do not further reduce the symmetry from $P4_32_12$. In Eq. (2) the lowest degree invariants which couple Γ_1^+ and Γ_3^+ respectively with X_4 are shown. Here, Γ_1^+ implies a dilatational (or compressional) strain and Γ_3^+ a tetragonal and/or orthorhombic strain

$$\begin{aligned}\Delta F_\lambda = {} & \lambda_1 \psi(\eta_1^2+\eta_2^2+\eta_3^2+\eta_4^2+\eta_5^2+\eta_6^2) \\ & +\lambda_2[\phi_1(\eta_1^2+\eta_2^2-\tfrac{1}{2}\eta_3^2-\tfrac{1}{2}\eta_4^2-\tfrac{1}{2}\eta_5^2-\tfrac{1}{2}\eta_6^2) \\ & -\tfrac{3}{2}\phi_2(\eta_3^2+\eta_4^2-\eta_5^2-\eta_6^2)]. \qquad (2)\end{aligned}$$

The coupling coefficients are indicated by λ_1, λ_2, and the strain components take the symmetry adapted form $\psi \equiv \varepsilon_{11}+\varepsilon_{22}+\varepsilon_{33}$ for irreducible representation Γ_1^+ and

$$(\phi_1, \phi_2) \equiv \left(\frac{\varepsilon_{11}+\varepsilon_{22}-2\varepsilon_{33}}{\sqrt{3}}, \varepsilon_{11}-\varepsilon_{22}\right)$$

for irreducible representation Γ_3^+. Notice that both coupling terms are linear-quadratic in strain and primary order parameter respectively. For an unclamped (stress-free) crystal $\frac{\partial \Delta F_{tl}}{\partial \psi}=0$ and $\frac{\partial \Delta F_{tl}}{\partial \phi_i}=0$ where $\Delta F_{tl}=\Delta F + \Delta F_\lambda$ (see Eqs. (1) and (2)). By solving the homogeneous equations for ψ, ϕ_1, and ϕ_2 in terms of η, it is seen that the spontaneous strains depend quadratically upon the order parameter components. In particular, for the transition to $P4_32_12$, for domain (1), only η_1 and η_2 are non-zero and the resulting strain components are:

$$\begin{aligned}&\psi \propto (\eta_1^2+\eta_2^2);\\ &\phi_1 \propto (\eta_1^2+\eta_2^2);\\ &\phi_2 = 0. \qquad (3)\end{aligned}$$

Thus, a volumetric strain from ψ and a tetragonal strain from ϕ_1 occurs at the transition. As can be seen from the discussion by Lüthi and Rehwald (1981) ultrasonic studies should show a discontinuity in the elastic constants $C_{11}+2C_{12}$ and $C_{11}-C_{12}$, but not an elastic constant softening. This is due to the linear-quadratic coupling. Notice that ϕ_2 is zero and there is then no orthorhombic strain, as one would expect. Because the transition is first order, discontinuous jumps in modes C_{33}, C_{13} and C_{66} are also expected, as these modes are degenerate with C_{11}, C_{12}, and C_{44} respectively in the cubic phase.

Implausibility of the Proposed $I\bar{4}2d$ Structure for β-Cristobalite

Wright and Leadbetter (1975) and O'Keefe and Hyde (1976) proposed an ordered structure with subgroup symmetry $I\bar{4}2d$ for β-cristobalite. The averaged structure $Fd\bar{3}m$ was interpreted as being composed of "ideal" cristobalite with the space group symmetry of $I\bar{4}2d$ and the same primitive cell size. This relationship requires that the $I\bar{4}2d$ structure be determined by the onset of a primary order parameter at the Brillouin zone center. As can be seen from Stokes and Hatch (1988) the higher symmetry space group $Fd\bar{3}m$ allows a transition to the $I\bar{4}2d$ subgroup by the onset of a single primary order parameter transforming according to the Γ_5^- irreducible representation. The resulting $I\bar{4}2d$ structure is quite different from the known α-cristobalite structure. In Table 4 we give the three rotational modes for the irreducible representation Γ_5^-. Again, these modes are rotations around silicon atoms located at the centers of the tetrahedra. In a manner completely analogous to our development for the domains of $P4_32_12$, there are six positions around 16(c) points of the C9 structure which give the 96(h) positions. The correlated rotations of connected tetrahedra, however, are not equivalent to the rotations obtained for the domains of $P4_32_12$. In $I\bar{4}2d$, connected tetrahedral chains along $\langle 110\rangle$ directions are rotated about the *same* axis but with opposite angles ($\pm\theta$). Domain (2) of $I\bar{4}2d$ is shown in Fig. (5). At a local oxygen site both sets of domains (the $P4_32_12$ set and the $I\bar{4}2d$

Table 4. The three rotational mode components for the rigid SiO_4 tetrahedra

Mode	Points $(\frac{1}{8}, \frac{1}{8}, \frac{1}{8})$ $(\frac{7}{8}, \frac{3}{8}, \frac{3}{8})$	Points $(\frac{1}{8}, \frac{5}{8}, \frac{5}{8})$ $(\frac{7}{8}, \frac{7}{8}, \frac{7}{8})$	Points $(\frac{5}{8}, \frac{1}{8}, \frac{5}{8})$ $(\frac{3}{8}, \frac{3}{8}, \frac{7}{8})$	Points $(\frac{5}{8}, \frac{5}{8}, \frac{1}{8})$ $(\frac{3}{8}, \frac{7}{8}, \frac{3}{8})$
(1)	(0, 0, a)	(0, 0, a)	(0, 0, a)	(0, 0, a)
	(0, 0, −a)	(0, 0, −a)	(0, 0, −a)	(0, 0, −a)
(2)	(a, 0, 0)	(a, 0, 0)	(a, 0, 0)	(a, 0, 0)
	(−a, 0, 0)	(−a, 0, 0)	(−a, 0, 0)	(−a, 0, 0)
(3)	(0, a, 0)	(0, a, 0)	(0, a, 0)	(0, a, 0)
	(0, −a, 0)	(0, −a, 0)	(0, −a, 0)	(0, −a, 0)

The modes transform according to the irreducible representation Γ_5^-. (See Table 2 for further explanations)

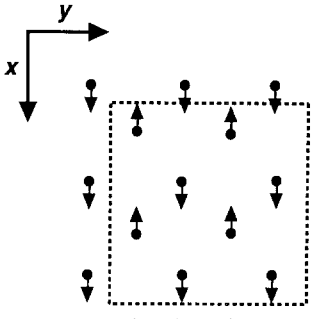

Fig. 5. Rotational mode pattern of rigid tetrahedra coordinating silicon atoms, resulting in the subgroup $I\bar{4}2d$, domain (2). Axial vectors are located at the 8(a) silicon atom positions of $Fd\bar{3}m$. The vectors indicate the direction of a right-handed rotation axis

set) give the same 96(h) positions, but the correlated motions along chains are basically different because they arise from distinct order parameters, X_4 versus Γ_5^-. In addition, the $P4_32_12$ group is not a subgroup of $I\bar{4}2d$ and therefore the relationship between them cannot be described by the onset of single or coupled order parameters.

Discussion

Observed Domain- and Micro-Structures in α-Cristobalite

The microstructures in α-cristobalite following the $\beta \rightarrow \alpha$ transition have been observed in the electron microscope by Christie et al. (1971) and Lally et al. (1978) in lunar rocks and by Withers et al. (1989) in a high temperature ceramic sample. Transformation twins with widely separated twin boundaries parallel to $\{110\}_c$ resulting from the loss of the three-fold rotation axes were readily observed. Antiphase domains with curved boundaries resulting from the loss of the translation vector $\frac{1}{2}\langle 011\rangle_c$ are also present. Lally et al. (1978) determined the displacement vector to be $\frac{1}{2}\langle 111\rangle_t$ and suggested that it indicates a $I\bar{4}2d \rightarrow P4_32_12$ or $P4_12_12$ transition. However, $\frac{1}{2}\langle 111\rangle_t \equiv \frac{1}{2}\langle 011\rangle_c$. Hence, this displacement vector is also consistent with the $Fd\bar{3}m \rightarrow P4_32_12$ or $P4_12_12$ transition we propose. Similar to the antiphase domain boundary, the boundary between two enantiomorphous twin domains is not crystallographically controlled because of lack of strain. Two contiguous tetragonal twin domains separated by a curved boundary observed by Withers et al. (1989) are most likely enantiomorphous domains.

In addition, closely spaced planar boundaries, nearly but not exactly parallel to $\{111\}_c$ were observed by Withers et al. (1989), the structural origin of which was not clear. Because the topology of the tetrahedral silica sheet in tridymite parallel to (001) is identical to that in cristobalite parallel to $\{111\}_c$, we suggest that these planar features are thin intercalated layers of tridymite in cristobalite. Such mixed-phases are well known in ceramic samples and result from the incomplete cristobalite to tridymite transition (cf. Thompson and Wennemer 1979).

The Si-O-Si Angle in α- and β-Cristobalite

Jackson and Gordon (1988) have shown that for α-cristobalite a rigid ionic model predicts the Si-O-Si angle to be 177.9°, close to the 180° value in ideal β-cristobalite. They used a shell model to successfully predict the α-cristobalite structure, in which the shells are allowed to shift toward the nearest two Si^{4+} cations and off the S-O bond axis. The predicted Si-O bond length (1.608 Å) and Si-O-Si angle (146°) are in good agreement with the experimental values found in α-cristobalite. From an *ab initio* quantum mechanical calculation of the covalent dimeric $H_6Si_2O_7$ molecule, Lasaga and Gibbs (1988) derived the bridging Si-O bond length (1.602 Å) and the Si-O-Si angle (144.2°), which are remarkably close to those in α-cristobalite. Hence, the basis for the Si-O-Si angle being 146° rather than 180° lies in the strong covalency of the Si-O bonds in α-cristobalite. Therefore it is safe to assume that the Si-O-Si angle remains unchanged through the α-β cristobalite transition.

Microscopic Mechanism and Dynamics of the α-β Transition in Cristobalite

Dynamic structure of β-cristobalite. We have already discussed in detail the distinct domains, which result from the $\beta \rightarrow \alpha$ transition. In α-cristobalite, these domains are large (macroscopic) and static, whereas in β-cristobalite they are microscopic and dynamic. In either case, all domains are energetically equivalent. Hence, the β-phase can be described in terms of a potential well with twelve identical minima with a fairly low energy barrier in between, such that the microscopic domains can be described as resonating among the twelve distinct domain configurations. Because the coupled tetrahedral rotations occur in columns parallel to $\langle 110\rangle$ in the cubic β-phase (Fig. 4), the correlation length of the dynamic domains is long parallel to $\langle 110\rangle$. The intense diffuse scattering in sheets normal to $\langle 110\rangle$ observed in the electron diffraction pattern of β-cristobalite (Hua et al. 1988) is in very good agreement with this dynamic structure. The small enthalpy of fusion (8.9 ± 1.0 kJ/mole) of cristobalite (Richet et al. 1982) may be explained by the dynamical structure of the β-phase. Since cristobalite is the least dense among the silica polymorphs, structure of molten silica may very well consist of finite fluctuating clusters of α-cristobalite.

Fluctuations and Crossover from the Displacive to the Order-Disorder Regime. As mentioned earlier, the primary order parameter, which transforms as the X_4 representation, consists of simultaneous rotation and translation of the silicate tetrahedra along the x and y axes. Since the tetrahedral rotation and translation are linearly related by symmetry, in α-cristobalite deviation of the observed Si-O-Si angle from 180° (ΔSi-O-Si) can be used as a measure of the order parameter. In fact, the experimental Si-displacement and ΔSi-O-Si angle are linearly related (Fig. 6). In Fig. 7, the ΔSi-O-Si angle is plotted against temperature from the data obtained from structure reinements of α-cristobalite by Peacor (1973) and Pluth et al. (1985). It is seen that the (first-order) phase transition at T_o ($\sim 220°$ C) initiates long before the ΔSi-O-Si angle approaches a zero value. This abrupt transition from α- to the β-phase is due to the energetically unfavorable 180° Si-O-Si angle required by the ideal C9 structure.

Hence, the displacive regime in α-cristobalite is very limited and at T_o, there is a crossover to the order-disorder mechanism, whereby different domain configurations dynamically interchange due to statistical fluctuations. These fluctuations are hydrodynamic in nature and result from a coupling of the order parameter with strain. Hence, the optic mode which transforms as the

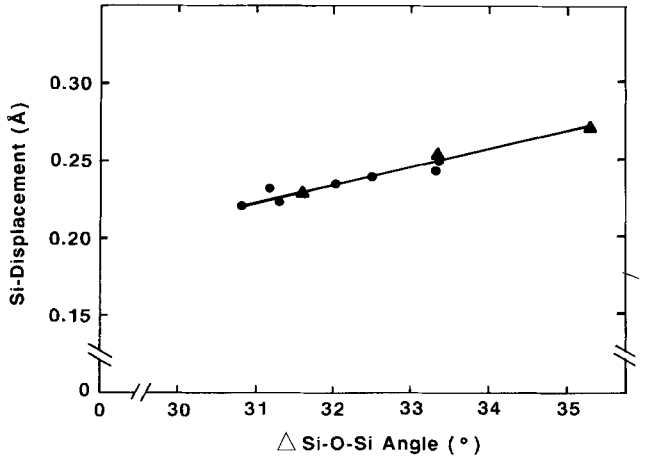

Fig. 6. Linear relation between the Si-displacements from the ideal C9 structure and the deviation of Si-O-Si angle from 180° (*Δ*Si-O-Si) in α-cristobalite (triangles: Pluth et al. 1985; circles: Peacor 1973)

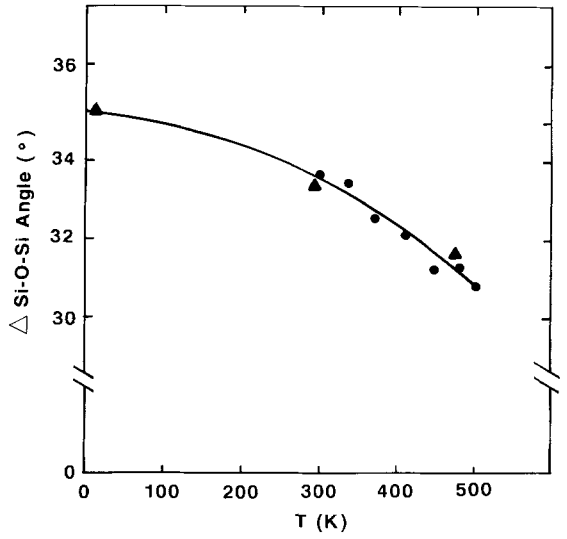

Fig. 7. The deviation of the Si-O-Si angle from 180° (*Δ*Si-O-Si) as a measure of the order parameter, plotted against temperature in α-cristobalite (triangles: Pluth et al. 1985; circles: Peacor 1973)

primary order parameter, couples with strain; a change in the elastic constants sum $\frac{1}{2}$ (C_{11}-C_{12}) should appear and fluctuations in the primary order parameter should be evidenced in the appropriate acoustic modes near k = 0.

With increasing temperature above T_o, the domain size (correlation length) will decrease and the fluctuation frequency will increase. But at no temperature, however high, the β-phase will ever attain the ideal C9 structure because of the energetically unfavorable 180° Si-O-Si angle mentioned earlier. Hence, the α-β transition in cristobalite is an interesting case, where the second-order nature of the transition is allowed by the Landau criterion, but forbidden because of (stereochemical) structural reasons, explaining the fluctuation-induced first-order character of the α-β transition.

Acknowledgement. This research has been supported by the National Science Foundation (EAR-8719638).

References

Aizu K (1970) Determination of state parameters and formulation of spontaneous strain for ferroelectrics. J Phys Soc Jpn 28:706–716

Christie JM, Lally JS, Heuer AH, Fisher RM, Griggs DT, Radcliffe SV (1971) Comparative electron petrography of Apollo 11, Apollo 12, and terrestrial rocks. Proc Second Lunar Sci Conf 1:69–89, MIT Press

Dollase WA (1965) Reinvestigation of the structure of low cristobalite. Z Kristallogr 121:369–377

Fischer R, Zemann J (1975) Geometrische und elektrostatische Berechnungen am Quarz und am Cristobalit-Typ. I. Modelle mit AB_4-Tetraedern der Symmetrie $\bar{4}3m$. Tschermaks Mineral Petrogr Mitt 22:1–14

Hua GL, Welberry TR, Withers RL, Thompson JG (1988) An electron diffraction and lattice dynamical study of the diffuse scattering in β-cristobalite, SiO_2. J Appl Crystallogr 21:458–465

Jackson MD, Gordon RG (1988) MEG investigation of low pressure silica shell model for polarization. Phys Chem Minerals 16:212–220

Lally JS, Nord GL Jr., Heuer AH, Christie JM (1978) Transformation-induced defects in α-cristobalite. Proc Ninth Int Cong Electron Microscopy 1:476–477

Lasaga AC, Gibbs GV (1988) Quantum mechanical potential surfaces and calculations on minerals and molecular clusters I. STO-3G and 6-31G* results. Phys Chem Minerals 16:29–41

Leadbetter AJ, Wright AF (1976) The α-β transition in the cristobalite phases of SiO_2 and $AlPO_4$ I. X-ray results. Philos Mag 33:105–112

Lüthi B, Rehwald W (1981) Ultrasonic studies near structural phase transitions. In: Müller KA, Thomas H (eds) Structural Phase Transitions I. Springer, Berlin Heidelberg New York, pp 131–184

Miller SC, Love WF (1967) Tables of Irreducible Representations of Space Groups and Co-Representations of Magnetic Space Groups. Pruett, Boulder

Nieuwenkamp W (1937) Übr die Struktur von Hoch-Cristobalit. Z Kristallogr 96:454–458

O'Keefe M, Hyde BG (1976) Cristobalites and topologically-related structures. Acta Crystallogr B32:2923–2936

Peacor DR (1973) High-temperature single crystal study of the cristobalite inversion. Z Kristallogr 138:274–298

Pluth JJ, Smith JV, Faber J Jr (1985) Crystal structure of low cristobalite at 10, 293, and 473 K: variation of framework geometry with temperature. J Appl Phys 57:1045–1049

Richet P, Bottinga Y, Denielou L, Petitet JP, Tequi C (1982) Thermodynamic properties of quartz, cristobalite and amorphous SiO_2: drop calorimetry measurements between 1000 and 1800 K and a review from 0 to 2000 K. Geochim Cosmochim Acta 46:2639–2658

Sapriel J (1975) Domain wall orientations in ferroelastics. Phys Rev B12:5128–5140

Stokes HT, Hatch DM (1988) Isotropy Subgroups of the 230 Crystallographic Space Groups. World Scientific, Singapore

Thompson AB, Wennemer M (1979) Heat capacities and inversions in tridymite, cristobalite, and tridymite-cristobalite mixed phases. Am Mineral 64:1018–1026

Van Valkenburg A Jr, Buie BF (1945) Octahedral cristobalite with quartz paramorphs from Ellora Caves, Hyderabad State, India. Am Mineral 30:526–535

Welberry TR, Hua GL, Withers RL (1989) An optimal transform and Monte Carlo study of the disorder in β-cristobalite. J Appl Crystallogr 22:87–95

Wright AF, Leadbetter AJ (1975) The structures of the β-cristobalite phases of SiO_2 and $AlPO_4$. Philos Mag 31:1391–1401

Wyckoff RWG (1925) The crystal structure of the high temperature form of cristobalite (SiO_2). Am J Sci 9:448–459